UNIVERSITY OF DUNDEE

University of Dundee

An early developmental vertebrate model for nanomaterial safety

Webster, Carl A.; Di Silvio, Desire; Devarajan, Aarthi; Bigini, Paolo; Micotti, Edoardo; Giudice, Chiara; Salmona, Mario; Wheeler, Grant N.; Sherwood, Victoria; Bombelli, Francesca Baldelli

Citation for published version (APA):
Webster, C. A., Di Silvio, D., Devarajan, A., Bigini, P., Micotti, E., Giudice, C., ... Bombelli, F. B. (2016). An early developmental vertebrate model for nanomaterial safety: Bridging cell-based and mammalian toxicity assessment. Nanomedicine, 11(6), 643-656. DOI: 10.2217/nnm.15.219
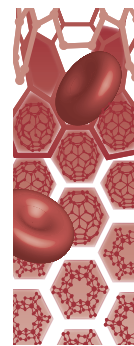
An early developmental vertebrate model for nanomaterial safety: bridging cell-based and mammalian toxicity assessment

Aim: With the rise in production of nanoparticles (NPs) for an ever-increasing number of applications, there is an urgent need to efficiently assess their potential toxicity. We propose a NP hazard assessment protocol that combines mammalian cytotoxicity data with embryonic vertebrate abnormality scoring to determine an overall toxicity index. **Results:** We observed that, after exposure to a range of NPs, *Xenopus* phenotypic scoring showed a strong correlation with cell based *in vitro* assays. Magnetite-cored NPs, negative for toxicity *in vitro* and *Xenopus*, were further confirmed as nontoxic in mice. **Conclusion:** The results highlight the potential of *Xenopus* embryo analysis as a fast screening approach for toxicity assessment of NPs, which could be introduced for the routine testing of nanomaterials.

Carl A Webster[1], Desire Di Silvio[1], Aarthi Devarajan[1], Paolo Bigini[3], Edoardo Micotti[3], Chiara Giudice[4], Mario Salmona[3], Grant N Wheeler[2], Victoria Sherwood**[,1,5] & Francesca Baldelli Bombelli*[,1,6]

[1]School of Pharmacy, University of East Anglia, Norwich, UK
[2]School of Biological Sciences, University of East Anglia, Norwich, UK
[3]IRCCS-Istituto di Ricerche Farmacologiche 'Mario Negri', Milan, Italy
[4]DIVET, Università degli Studi di Milano, Milan, Italy
[5]Skin Tumour Laboratory, Jacqui Wood Cancer Centre, University of Dundee, Dundee, UK
[6]Department of Chemistry, Materials and Chemical Engineering "G.Natta", NFMLab, Politecnico di Milano, Milan, Italy
*Author for correspondence: francesca.baldelli@polimi.it
**Author for correspondence: sherwood@dundee.ac.uk

Background

Objects at nanoscale (<100 nm) take on novel characteristics due to their small size and extensive surface area, providing markedly different properties to develop reagents for biomedicine. As such, nanomaterials are being developed for an ever-increasing number of diseases including; infectious diseases, hepatitis, cardiac and vascular disorders, immune and degenerative diseases, and cancer [1]. However, their high surface area-to-volume ratio renders nanoparticles (NPs) highly reactive, which can result in toxicity within biological systems [1–3]. At present a dedicated regulatory framework for testing nanomedicines does not yet exist and cell-based assays are the current method of choice despite poor *in vitro-in vivo* correlations of nanomaterial toxicity [4]. Despite the increase in number of publications in nanomedicine over the past 5–10 years [5,6], it is often difficult to obtain conclusive results on the toxicity of engineered nanomaterials, which is due to poor physico–chemical characterization of the material and a distinct lack of standardized protocols [7]. This is seriously hampering the transfer of many promising nanomedicines to the clinic.

Safety assessment is a necessary step in the process to develop a novel nanomedicine and should involve further refinement at early stages in NP development to guarantee appropriate safety. Learning from the development of first-generation nanomedicines that have been used in clinical procedures for years [8] and have been tested using the standard procedures for the evaluation of all drugs [9], it is desirable to develop methods that are tailored to evaluating specific toxicities associated with nanomaterials. Recently, much effort from the nanocommunity has been directed to optimize protocols that assess the safety of nanomaterials. This concept is known as 'safety by design' [5] and is crucial for the production of nanomedicines, for which engineering at the nanoscale can

Future Medicine part of fsg

Figure 1. Nanotoxicity screening assay workflow. A novel NP is characterized in assay buffers, cell (RPMI) and embryo (0.1 × MMR) culture media. Unstable or aggregating NPs can be redesigned or altered through surface modifications. Once a stable NP is fully characterized, an integrated protocol combining cytotoxicity screens in a range of cell types (cell viability and cell stress) and *Xenopus laevis* ranking of phenotype abnormalities is applied in parallel. The results are combined to produce a score that indicates if the NPs should be applied in a rodent model and further developed for pharmaceutical use.
MMR: Marc's modified ringers; NP: Nanoparticle.

cause unpredictable biological responses [10]. A compromise has to be met in order to produce nanoma-terials with desired properties (which for targeted treatments are often multifaceted, complex formula-

tions), with tolerable toxicity and thus there is a need for robust screening methodologies at an early stage in NP development. Currently, the field requires a system that can bridge the safety assessment of NPs in cell-based assays with reliable data generated from mammalian *in vivo* toxicity assessment, providing stronger correlations between the two toxicological models.

A preclinical screening tool that effectively assesses toxicity of nanomedicines prior to mammalian models will enormously reduce the number of materials that need to be tested in higher vertebrate systems, while also improving the success rates of novel nanomaterials to pass mammalian toxicity assessment models. Most new generation nanomedicines are multicomponent systems with complex chemical structures, joining the properties of different materials in one unique engineered object, often involving the use of non-FDA approved materials. Therefore, there is a clear need to test the toxicity of the engineered nano-object at different stages of production. Thus, one consequence of generating multicomponent NPs for biomedical purposes is the potential of having to use a larger number of mammals for safety assessment than for the development of conventional drugs. It would be advantageous to test NP toxicity using a system that can bridge the gap in generating consistent data between *in vitro* cell-based assays and mammalian models of toxicity assessment [11,12]. Early developmental vertebrate models such as *Danio rerio* (zebrafish) and *Xenopus laevis* (African clawed frog) provide rapid and inexpensive systems for NP toxicity assessment, compared with adult mammalian models [11,13–15]. *X. laevis* produce embryos in sizeable quantities (adaptable for high-throughput screening) that are relatively large (~1 mm in diameter at early stages of embryonic development), making them highly suitable *in vivo* systems for the assessment of toxicants. *X. laevis* has a long-running history in toxicity testing, such as the frog teratogenesis assay-*Xenopus* (FETAX), which provides strong prediction of teratogens in mammals [16]. In addition they provide a means to investigate the toxicity of materials on whole organs, post organogenesis, to better simulate an adult model. Further advantages of using *X. laevis* as an *in vivo* toxicity model, include external development of the embryo to allow for temporal control over the exposure to NPs and facilitating investigation into toxic effects at critical stages of embryogenesis, such as gastrulation and neuralation. Furthermore, *X. laevis* developmental stages are well characterized making it an ideal model for phenotypic assays [17,18]. The sensitivity of embryos during development can be exploited to identify varying degrees of toxicity by a range of phenotypic abnormalities, providing

an indication into safe dosages; information that historically is not accurately known before assessment in mammalian models.

In this study, we propose to use *X. laevis* embryos in combination with *in vitro* testing in mammalian cell lines to provide a multitiered, rapid and low cost approach to assess NP toxicity prior to *in vivo* mammalian testing. We have developed a methodology that assesses the toxicity of nanomaterials at an early stage in their production, before further assessment for translational applications (Figure 1). The methodology combines a full physicochemical characterization of the nanomaterial with quick and inexpensive *in vitro* cytotoxicity assays, and analysis in *X. laevis* embryos at different developmental stages, prior to mammalian testing.

Methods

NP synthesis & characterization

NH_2-Fe_3O_4 and PS-COOH NPs were commercially available and therefore bought from Nanocs (product code MP25-AM) and Invitrogen (product code F-8887), respectively. CdSe QDs and PEG-Fe_3O_4 NPs were synthesized in-house. All NPs were fully characterized as described in the Supplementary Information. In addition, details about cell culture, all mouse procedures and statistical information is provided in the Supplementary Section.

Trypan blue exclusion assay

Cells were cultured as described in the Supplementary Information. A549 and SK-MEL-28 lines were seeded at 26,550 cells/ml and MDCK at 20,000 cells/ml in 24 well-plates for trypan blue exclusion assay, which was carried out as previously described [19]. After attachment overnight, cells were exposed to different concentrations of NPs for 72 h before analysis.

MTT assay

Cell viability after exposure to NPs was assessed by MTT, as previously described [20]. Cells were seeded in 96-well plates at an initial density of 4500 cells/well and exposed to NPs for 72 h. Cell viability was calculated as a ratio of mean absorbance from quadruplicate readings, normalized to nonstimulated cells.

Immunoblotting

Cells were lysed in 50 mM Tris-HCl (pH 7.5), 1% Triton X-100, 150 mM NaCl and spun at 16,000 x *g* for 30 min at 4°C. Immunoblotting was performed as previously described [21] using 1:1000 anti-PARP-1 (Santa Cruz Biotechnology) and 1:5000 anti-rabbit (Cell Signaling) antibodies, in 5% BSA.

X. laevis phenotypic assay

All experiments were performed in compliance with the relevant laws and institutional guidelines at the University of East Anglia. The research has been approved by the local ethical review committee according to UK Home Office regulations. *X. laevis* embryos were obtained as previously described [22,23]. Embryos were staged using the Nieuwkoop and Faber (NF) normal table of *Xenopus* development [24]. Embryos developed at 18°C until they reached the required stage. Embryos (5 per well) were placed in a 24-well plate and exposed to NPs. Once at the required stage, embryos were washed twice with PBS before fixing in MEMFA (3.7% formaldehyde 1 × MEM salts, MQW [1:1:8]) overnight at 4°C. A further two PBS washes of the embryos was performed before embryos were scored for phenotypic abnormalities.

X. laevis whole mount florescence microscopy

NF stage 38 *X. laevis* embryos were exposed to 10^{15} NP/ml PS-COOH until NF stage 45 and anaesthetized with 0.6 mg/ml ethyl 3-aminobenzoate methanesulfonate salt (Sigma Aldrich). PS-COOH NPs were imaged in the bloodstream of anaesthetized embryos using Nikon Eclipse 600 with a CCD digital camera, with an emission filter of 509–547 nm.

X. laevis transmission electron microscopy (TEM) imaging

Embryos exposed to $10^{15.3}$ NP/ml PEG-Fe$_3$O$_4$ during NF stage 38 to NF stage 45 were euthanized, fixed, embedded and sectioned as previously described [25]. Sections were observed using a Tecnai 20 TEM with AMT cameras, operating at an acceleration voltage of 200 kV.

Results

NP synthesis & characterization

Our proposed nanotoxicity testing protocol (Figure 1) has been tested using four different NPs; CdSe quantum dots (QD) NPs, pegylated magnetite NPs (Fe$_3$O$_4$-PEG), amine-functionalized magnetite NPs (Fe$_3$O$_4$-NH$_2$) and fluorescent carboxylated polystyrene NPs (PS-COOH), selected for: a putative highly toxic NP as a positive control (QDs); two iron-oxide NPs (possible MRI contrast agents), with different surface functionalization and physical chemical stability to test the ability of the protocol to detect potential differences in toxicity based on NP modifications [26,27]; and a negatively charged NP (PS-COOH) [28], being part of the first group of materials to be evaluated for safety at the nanoscale. Both QD and Fe$_3$O$_4$-PEG NPs were synthesized and purified in-house as explained in the material and methods section, while PS-COOH and Fe$_3$O$_4$-NH$_2$ NPs were bought from specific suppliers and further characterized.

NP characterization is an essential first step in our protocol design (Figure 1). TEM and mean core sizes for the NPs are reported in Table 1, while statistical analysis of the size together with representative images are shown in Supplementary Figure 1 in the Supplementary data section. NPs were also characterized by dynamic light scattering (DLS) and ζ-potential in aqueous dispersions (except for the Fe$_3$O$_4$-PEG NPs that were dispersed in PBS) which showed that hydrodynamic diameters were generally larger than TEM core sizes and that hydrodynamic sizes for QD and Fe$_3$O$_4$-NH$_2$ NPs indicated the formation of NP clusters to some extent (Supplementary Figure 2A). NP stability and aggregation behaviors were studied in the embryo (0.1× Marc's modified ringers [MMR]) and cell growth media (RPMI + 10% FBS) over 72 h, where the results at the starting time for the highest concentration measured are reported in Table 1. PS-COOH and Fe$_3$O$_4$-PEG NPs were stable, while QD and Fe$_3$O$_4$-NH$_2$ showed extensive aggregation at this concentration, however, aggregation was less extensive at lower concentrations for both NPs, demonstrating that further biological investigation was possible for all the NPs selected. NP hydrodynamic sizes in the differ-

NP	TEM (nm)	Water/PBS		Zeta potential (mV)	RMPI-1640 10% FBS		0.1 × MMR	
		HDS (nm)	PDI		HDS (nm)	PDI	HDS (nm)	PDI
QD	4.5 ± 2.0	21.4 ± 1.5	0.1	-27.4 ± 0.0	107.5 ± 1.2	0.7	122 ± 1.5	0.1
PEG-Fe$_3$O$_4$	6.4 ± 1.2	21.9 ± 0.1	0.2	-3.9 ± 0.8	32.9 ± 3.0	0.2	22.1 ± 0.9	0.2
PS-COOH	22.6 ± 5.6	34.5 ± 0.7	0.2	-37.2 ± 2.0	75.4 ± 0.7	0.2	34.7 ± 0.7	0.2
NH$_2$-Fe$_3$O$_4$	11.3 ± 2.9	90.0 ± 0.5	0.2	+30.3 ± 3.8	294.0 ± 2.3	0.4	2268 ± 96	0.2

Table 1. Structural parameters of the nanoparticles from transmission electron microscopy and dynamic light scattering measurements.

FBS: Fetal bovine serum; HDS: Hydrodynamic diameter; MMR: Marc's modified ringers; NP: Nanoparticle; PDI: Polydispersity index; QD: Quantum dot.

ent environments were monitored over the experimental time for biological analysis and remained consistent as shown in Supplementary Figure 2B.

Cytotoxicity assessment analysis

We used a diverse array of mammalian cell types for cytotoxicity analysis (A549 [lung adenocarcinoma], SK-MEL-28 [melanoma] and MDCK [immortalized kidney] cells; that represent commonly available lines), which were exposed to varying concentrations of NPs over 72 h. After NP stimulation, trypan blue exclusion assay, MTT assay and protein expression of full and cleaved poly (ADP-ribose) polymerase-1 (PARP-1) were performed to evaluate cytotoxic effects. Figure 2 shows the cytotoxic effects the NP panel in the three cell types, as a function of exposure concentration expressed as NP/ml (for clarity analog graphs are reported vs concentration with different metrics [w/v and surface area/v] shown in Supplementary Figure 3, with representative images of the treated cells at the highest concentration of NP treatment shown in Supplementary Figure 4). As expected, QDs were highly toxic in all cell types for concentrations $>10^{14}$ NP/ml, which corresponds to a weight concentration of 0.1 µg/ml. The MTT results showed that exposure to the highest concentrations of Fe_3O_4-NH_2 and PS-COOH NPs on MDCK cells resulted in a 40% reduction in cell viability when compared with the other lines, while trypan blue results also showed reduced cell viability for the highest concentration of Fe_3O_4-NH_2. PARP-1, activated by the production of reactive oxygen species (ROS), is a substrate for active cysteinyl-aspartate protease cleavage and is a marker of apoptotic cell death [29]. Previous studies have suggested an increase in ROS production after exposure to nanomaterials [30–32]. We investigated PARP-1 cleavage in the cells in response to NP treatment and found that only QDs induced apoptosis in cells at a comparable concentration to that of the cytotoxic drug, cisplatin, while no cleaved PARP-1 was observed in cells incubated with the other NPs (Figure 2C). Taken together these *in vitro* findings show that QDs induced high levels of cytotoxicity in mammalian cells compared with the other NPs tested.

Xenopus laevis as a multiparametric nanotoxicity assessment tool

Xenopus laevis embryos at different stages of development were exposed to varying concentrations of NPs and morphological scoring of an array of phenotypic abnormalities was carried out (Figure 3A & Supplementary Figure 5). Phenotypic abnormalities were scored and used to assess the NP effect on the development of 30 embryos at all three of the selected

stages. Common abnormalities recorded included; edema, blistering, eye deformities, loss of melanocytes, tail loss, stunted growth, axial defects such as bent spines, degradation of tissue and developmental delay (Figure 3A & B & Supplementary Figure 5). Based on these abnormalities embryos were scored collectively as nonabnormal (healthy), abnormal or dead. By enabling all abnormalities to be marked in one category, simplifies the scoring system and keeps subjectivity between users to a minimum. Gastrulation occurs at an early phase of vertebrate development (in *Xenopus* at NF stage 10) and is a highly sensitive time to environmental changes during embryonic development, so to assess NP effects during this phase of development, embryos were exposed to the NPs at NF stage 4 and left to develop until NF stage 38 (Figure 3C). Another critical developmental process is neurulation, which occurs before organogenesis and gives rise to precursor tissues of the spinal cord, brain and neural crest [33]. To assess NP effects during neurulation and before organogenesis, embryos were exposed to the NPs at NF stage 15 and left to develop until NF stage 38 (Figure 3D). Finally, for *in vivo* embryonic systems that can more accurately represent an adult system, embryos were exposed to NPs at tadpole stages during organogenesis, specifically at NF stage 38–45 (Figure 3B & E). QDs showed severe toxicity in *X. laevis* embryos at all stages, which is in good agreement with mammalian developmental systems [34], and our cytotoxicity data (Figure 2). The other NPs had limited toxicity, with the Fe_3O_4-NH_2 and PS-COOH NPs showing toxic effects only at higher concentrations, while the Fe_3O_4-PEG NPs (synthesized in our laboratory as potential theranostic NPs), showed no toxicity at all stages, which is also in accordance with our *in vitro* findings (Figure 2).

We wanted to check that NPs exhibiting low-to-no toxicity in *X. laevis* embryos (iron oxide and PS-COOH NPs) were taken up into the embryos following exposure. Embryo uptake by the iron oxide NPs and PS-COOH NPs was monitored by TEM imaging of embryo sections at NF stage 45 (Supplementary Figure 6) and fluorescence microscopy (FM) of live embryos at NF stage 45 (Supplementary Figure 7), respectively. TEM analysis demonstrated the presence of the NPs in embryo tissues for both iron oxide NPs (Supplementary Figure 6). FM of intact embryos treated with PS-COOH NPs permitted us to detect their presence within the embryos, where NP uptake was proportional to exposure (Supplementary Figure 7). Moreover, videos (Movie) of anesthetized embryos showed PS-COOH NPs (or agglomerates) moving through embryonic intersomatic blood vessels (from which time frame stills over 0.70 s have been extracted and are shown in Supplementary Figure 7B). Importantly,
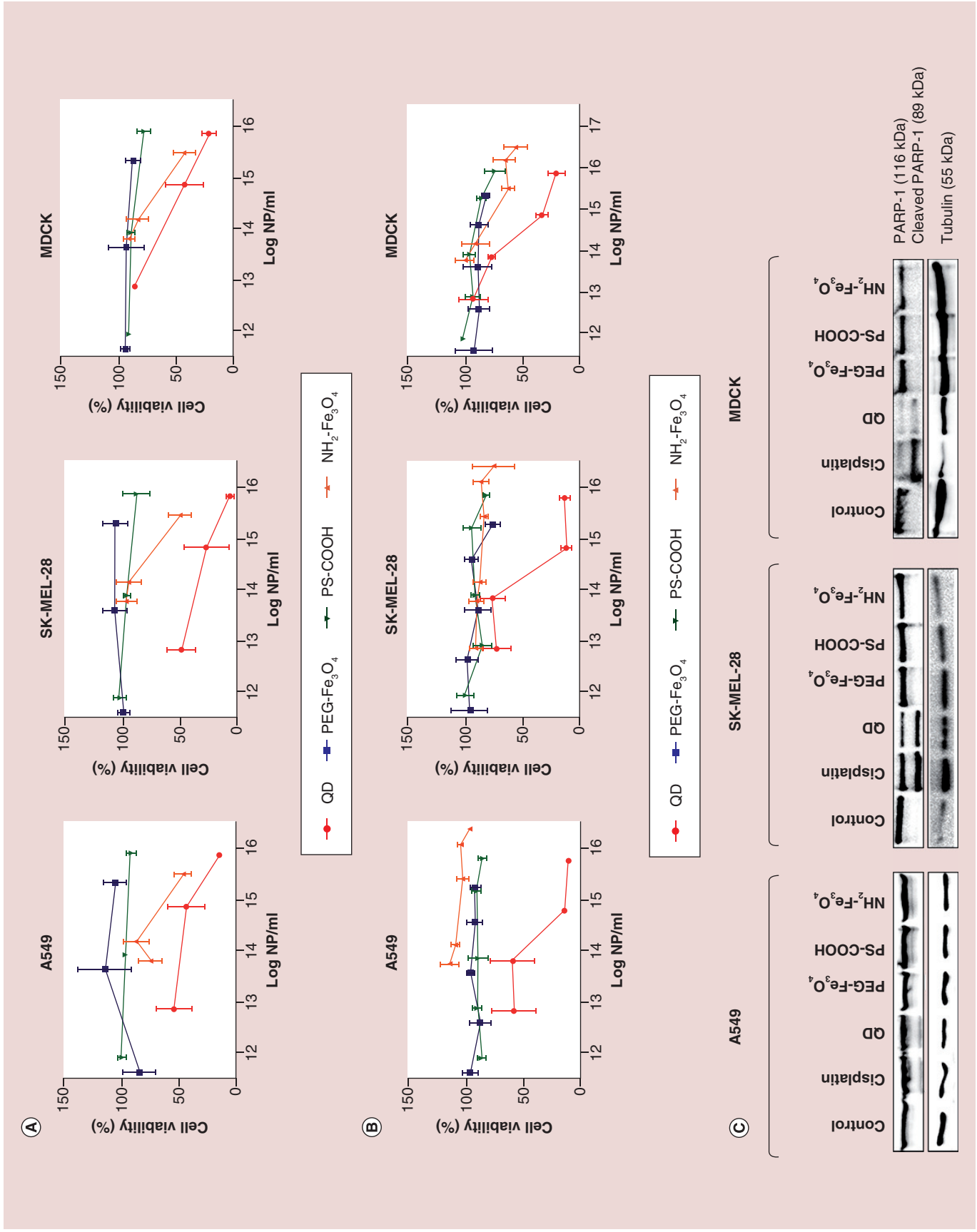
Figure 2. Evaluation of nanoparticle cytotoxicity (please see facing page). (A & B) A549, SK-MEL-28 and MDCK cell lines were exposed to varying concentrations of QD, PEG-Fe_3O_4, PS-COOH and NH_2-Fe_3O_4. After 72 h stimulation with NPs, trypan blue exclusion assay (A) and MTT assay (B) was performed to assess cell viability. Values represent mean ± SEM. MTT data also represented as alternative concentration indices (Supplementary Figure 3). **(C)** Protein expression of full length and cleaved PARP-1 in mammalian cell lines. Cells were stimulated for 24 h with 70 μM cisplatin (positive control), $10^{15.8}$ NP/ml QD, $10^{15.3}$ NP/ml PEG-Fe_3O_4, $10^{15.9}$ NP/ml PS-COOH and $10^{15.5}$ NP/ml NH_2-Fe_3O_4. Control cells were vehicle treated. β-tubulin was used as a loading control.
NP: Nanoparticle; QD: Quantum dot.

these data show that the NPs used in this study are readily taken up by the *X. laevis* embryos.

Comparison of cytotoxicity & *X. laevis* data for hazard ranking of NPs

We developed a logical ranking system for correlating cytotoxicity and *X. laevis* results, to provide an overall hazard score from each assay for the investigated NPs (Tables 2 & 3). For the cytotoxicity data the hazard score was obtained for the highest NP concentration, while for the *X. laevis* analysis we only took into account the results generated from the tadpole stage (Figure 3E; NF 38–45, when the embryo has fully formed organs and therefore the evaluation of nanotoxicity is more physiologically relevant to adult tissues). The obtained hazard indices are reported in Tables 2 & 3, which evaluates correlations between *in vitro* and *in vivo* results. The assays fully agreed on the evaluation of the toxicity for the highly toxic QDs that scored for severe toxic effects in all assays, as well as for the two iron oxide NPs that showed limited toxicity. However, PS-COOH NPs did not affect cell viability by the *in vitro* assays (Figure 2), yet exhibited toxicity effects at high concentrations as well as some moderate toxicity at lower concentrations in *Xenopus* (Figure 3). This suggests that the introduction of a *X. laevis* sampling test early on in NP development could help to identify false negatives for toxicity assessment produced by cell-based assays.

Assessment of NP safety in a mammalian system

In our protocol (Figure 1) if NP-induced developmental defects are observed in the *X. laevis* model, the NP will not progress to further assessment, rather only those nanoformulations that give no-to-low toxicity will progress to evaluation in small rodent models (in our data this was the two iron oxide NPs; Figures 2 & 3 & Tables 2 & 3). To validate the low-to-no toxic prediction of the iron oxide NPs, we administered these two NPs in mice to assess toxicity effects on the tissues where they accumulated (the target organs). For iron oxide core NPs, murine target organs could be easily identified using MRI analysis. MRI analysis showed that in T2-weighed MRI coronal slices from epigastric and mesogastric regions, both iron oxide NPs accumulated in the liver and kidneys of the NP-treated animals compared with vehicle-treated controls

(Figure 4A & B). Importantly, postmortem histological sections from the tissues where these NPs accumulated (the liver and kidneys) demonstrated not only that the iron distribution (as assessed by Perl's staining) corroborated the MRI findings, but importantly also failed to reveal any evidence of morphological tissue toxicity (Figure 4C) highlighting that these NPs exhibit little-to-no toxicity in mammalian tissues. These findings show that *X. laevis* embryos are a useful tool to predict NP safety prior to administration and further testing in mammalian models.

Discussion & conclusion

With the growth of nanomedicines as therapies for disease management in the clinic, comes an ever increasing need to effectively assess how nano-sized therapeutics can effect biological systems and, in particular, systemic toxicity mechanisms [35]. As such, there has emerged a need for models that can produce effective toxicity data as a transition between 2D *in vitro* cell culture assays and expensive, often time-consuming *in vivo* mammalian models.

An alternative approach to mimic *in vivo* conditions has been to develop 3D and coculture *in vitro* cell-based models that better represent the organization of tissues compared with conventional 2D monocultures [36–41]. However, these tissue mimetic models are not without their limitations as they fail to recapitulate the complete systemic interactions present between organ systems *in vivo*, but rather focus on the development of individual, tissue-specific models. An early vertebrate developmental model can provide a complete *in vivo* model system, but with the added advantage of being a rapid toxicity assessment tool. Specifically, we have proposed the use of *X. laevis* as a readily available laboratory model to develop such a nanotoxicity screening tool (Figure 1). The protocol does not need to be limited to the exclusive use of *Xenopus* embryos, but rather can be easily extended to other commonly used developmental models such as the zebrafish model [11,42–44]. Amphibians share physiological traits common to all vertebrates, including mammals. Specific advantages of *Xenopus* as a model include; permeable skin, that they are tetrapods (therefore developing lungs and limbs), possessing all additional organs/tissues most commonly affected in human diseases (skin, sensory organs, lymphatic, nervous systems, kidneys, GI tract,
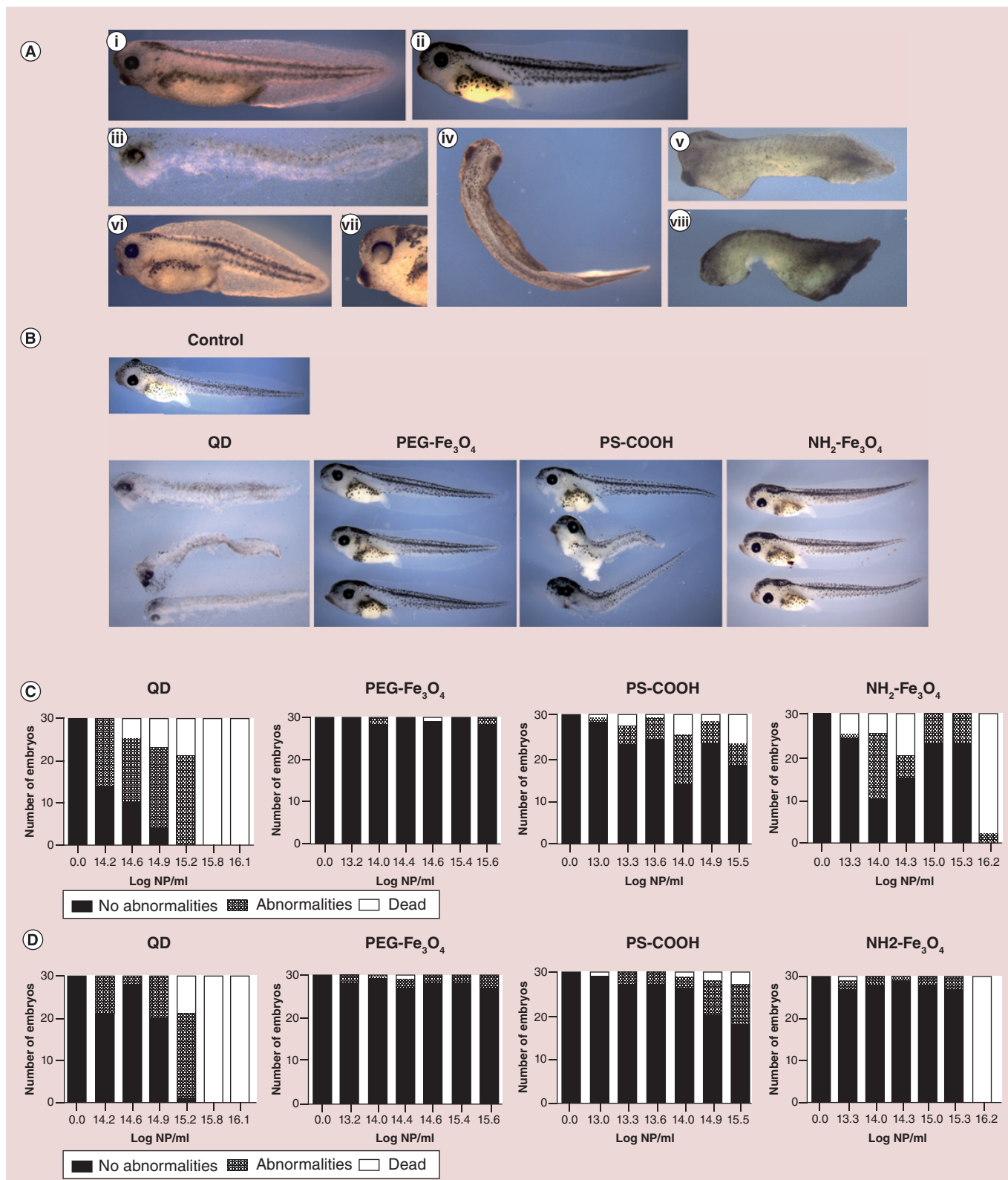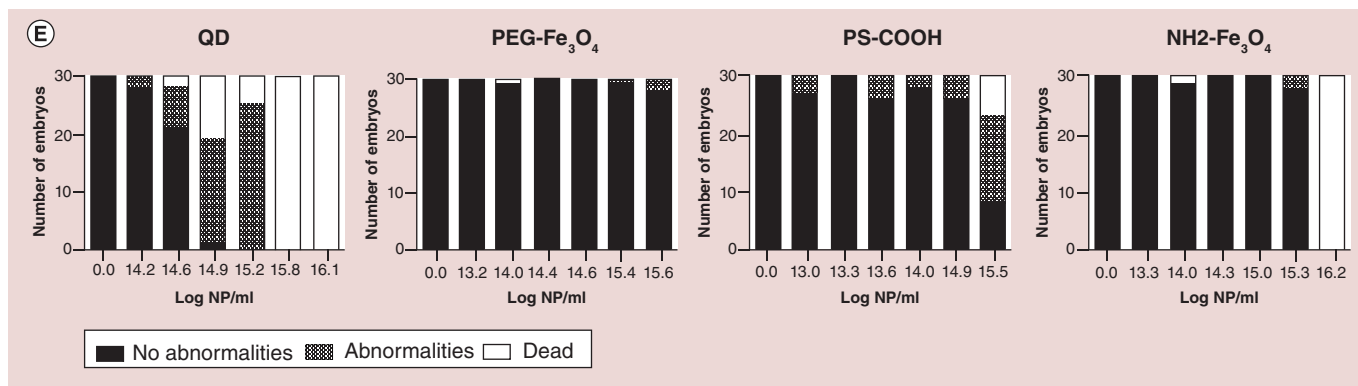
Figure 3. *Xenopus laevis* nanotoxicity phenotypic assay (for [A-D], please see facing page; for [E], please see above). (A) Representative images from the *X. laevis* phenotypic assay. **(Ai)** Control NF stage 38 embryo. **(Aii)** Control NF stage 45 embryo. **(Aiii)** embryo exposed to $10^{15.8}$ NP/ml QD at NF stage 38 and fixed at NF stage 45, all embryos were dead. **(Aiv)** Dorsal view of *X. laevis* with bent tail after exposure to $10^{14.2}$ NP/ml QD. **(Av & Aviii)***X. laevis* exposed to $10^{15.8}$ NP/ml QD at NF stage 4 and fixed when control embryos reached NF stage 38. Abnormalities include eye deformities, stunted growth/development, edema, blistering and melanocyte deformities. **(Avi & Avii)** Embryo exposed to $10^{14.2}$ NP/ml QD. Abnormalities include stunted growth, bent spin and loss of pigmentation in the eye. **(B)** Representative images embryos exposed to $10^{15.8}$ NP/ml QD, $10^{15.6}$ NP/ml PEG-Fe$_3$O$_4$, $10^{15.5}$ NP/ml PS-COOH and $10^{15.3}$ NP/ml NH2-Fe$_3$O$_4$. Embryos were developed in 0.1 × MMR and NP solution at different stages and fixed. The embryos were then analyzed for any developmental abnormalities or death. **(C–E)** Quantification of embryonic abnormalities. Histograms shown are of 30 embryos at each concentration of QD, PEG-Fe$_3$O$_4$, PS-COOH and NH$_2$-Fe$_3$O$_4$. *X. laevis* assessed as healthy (no abnormalities), developmental defects (abnormalities) and death (dead) as indicated, at different concentrations of NPs. Developmental defects include eye malformations, bent spine/tail, edema, blistering and stunted growth, as shown in **(A)**. **(C)** Embryos exposed at NF stage 4 and fixed at NF stage 38, **(D)** embryos exposed at NF stage 15 and fixed at NF stage 38 and **(E)** embryos exposed at NF stage 38 and fixed at NF stage 45.
NP: Nanoparticle; QD: Quantum dot.

cardiovascular, hepatic and circulatory systems), they are the highest evolutionary order providing free-living embryos to permit screening in multiwell formats, and in earlier life stages prior to the onset of independent feeding (before NF 45), they are described under the EU directive as not protected as nonhuman vertebrate models; thus making them highly amenable for toxicity testing procedures, as previously reviewed [18].

It is important that the physicochemical properties of the NPs are tested in the relevant biological fluids prior to toxicity assessment, so that the behavior of the NPs are well understood before proceeding to biological testing, enabling us to infer whether or not toxicity profiles are in fact dependent on the nanomaterial itself or NP aggregation. For example, the high salt concentration in the *X. laevis* embryo MMR buffer, affected the stability of electrostatically stabilized NPs such as QD and Fe$_3$O$_4$-NH$_2$ (Table 1), while the presence of proteins with further formation of protein-NP complexes [45] reduces aggregation in such NPs, suggesting that once *in vivo*, following initial exposure to aggregating NPs, this aggregation will likely be reduced in biological fluids.

In this study, we selected four NPs that span a variety of materials and presented different toxicity indices to test the suitability of this as a nanotoxicity protocol. Fe$_3$O$_4$-NH$_2$ NPs were found, according to our methodology, as having low-to-no-toxicity and further tested in mice with no evidence of any major acute toxicity

effect. We observed good agreement between *in vitro* and *in vivo* analysis for the nanomaterials tested, suggesting that there is a good correlation between nanotoxicity assessment in *X. laevis* and mammalian cells. The reputed toxic QD NPs and the iron oxide core NPs were ranked as toxic and low-to-no-toxicity, respectively, which is in agreement with data reported by others for similar NPs [46,47]. However, a significant contradiction in the ranking of the PS-COOH NPs was found between *in vitro* and *in vivo* results. Specifically, cytotoxicity was not detected in the investigated concentration range by any of the cell-based assays used, while mortality and abnormalities were scored for the embryos at higher PS-COOH NP concentrations, thus highlighting the importance of a fully integrated cell line and *X. laevis* approach to accurately assess nanomaterial safety and to identify false negatives. The physical characterization of PS-COOH NPs in biological fluids did not show any agglomeration effects that could promote toxicity. However, there is experimental evidence in the literature of toxicity effects due to carboxylic surface functionalization of polystyrene NPs is related to interaction with the blood plasma proteins [48,49]. FM on live embryos (Movie) confirmed the presence of high concentrations of PS-COOH NPs in the *X. laevis* tissues. Therefore, a fundamental step in our protocol is the comparison between the *in vitro* cytotoxicity data and the *in vivo* findings in *Xenopus* (Figure 1).

Table 2. Hazard score obtained from the cell assays and embryo analysis.

Hazard	Hazard score	Cell viability (%)	Healthy embryo (%)
0	0	>76	>76
x	1	50–75	50–75
xx	2	<50	<50

Moreover another toxicity aspect was tested, as the two chosen iron oxide NPs bearing specific surface functionalizations, showed different stability in the biological fluids at the highest concentration, where the Fe_3O_4-NH_2 NPs aggregated extensively. This concentration-dependent agglomeration was more pronounced in the MMR buffer than in cell growth media, promoting mortality of the embryos at the highest Fe_3O_4-NH_2 NP concentration, whereas no toxicity was observed for the lower concentrations at tadpole stages in the embryos (NF 38–45). This indicates that such a toxic effect was potentially related to the colloidal instability of the NPs rather than to the material composition of the NP itself. Instead, *in vitro* analysis provided mixed results depending on the cell line and of the assay that was used. Some toxicity was detected in the trypan blue exclusion assay at the highest concentration, which was not readily detectable in the MTT assay (Figure 2A & B). Of note, PARP-1 cleavage assay (Figure 2C) showed unambiguously no apoptosis for all the treated cell lines at the highest NP concentration, highlighting that numerous cytotoxicity assays are required in combination to effectively assess NP toxicity. Furthermore, cell line choice for nanotoxicity assessment provides a bespoke feature of this assay, where cell lines can be selected that are most suitable for analyzing nanomaterials designed for specific biomedical purposes.

For the *X. laevis* studies, we developed a simplified scoring system of the embryos allowing us to easily and rapidly assess NP-mediated toxicity in embryos at differing developmental stages (Figure 3C–E). We found that embryos exposed to PS-COOH NPs showed some toxicity for all stages at higher concentrations, in particular at the earliest stage (NF 4–38), where toxicity was observed from concentrations >10^{14} NP/ml. Embryos exposed to Fe_3O_4-NH_2 NPs showed toxicity at the earliest stage from concentrations >10^{14} NP/ml, while only at the highest NP concentration was 100% mortality observed at the other two stages of development. The severe toxicity observed at the highest concentration of Fe_3O_4-NH_2 NPs was related to the extensive aggregation of these NPs in MMR medium, which resulted in precipitation at high concentrations. However, at the latest stage (NF 38–45), for which the embryo has developed most of its organs, no toxicity was observed at all the other concentrations for Fe_3O_4-NH_2 NPs. Generally, we can state that where the embryos developed in the presence of NPs, NF stage 4 to NF stage 38 showed more phenotypic abnormalities and death at lower NP concentrations, than embryos exposed at NF stages 15 and 38. It is of note that between NF 38–45 the gills and mouth are open providing, in addition to the porous skin, possible respiratory and oral tract routes of exposure as well [50].

NPs were more toxic to embryos in early development (4–38 and 15–38 NF stages; Figure 3), in particular at the earliest stage, although it is difficult to say if this is connected to the different phase of development, or due to the longer exposure time to the NPs in these animals. While the first two stages might not be adaptable as prognostic model for toxicity in mammals, they can be used to evaluate teratogenesis. A study on *X. laevis* embryos, in which NPs were microinjected between NF stage 1 and 3, has shown that nanodiamond NPs with carboxylic surface groups promoted teratogenesis at both gastrulation and neurulation stages [51]. Other studies on *X. laevis* of metal oxide NPs (CuO, ZnO, etc.) have evaluated teratogenesis using the FETAX assay and reported major toxicity effects in the GI tract [14,25,52]. While FETAX focuses of teratogenic effects on midblastula stage embryos, we have demonstrated *X. laevis* as a versatile model that can be used to predict toxicity of nanomaterials beyond teratogenic effects.

Our protocol predicts that the combined cytotoxicity and *X. laevis* scores facilitate optimal prediction for toxicity in mammalian systems (Figure 1). Both iron core NPs gave a low hazard ranking for the cell culture

Table 3. Hazard score obtained from the cell assays and embryo analysis.

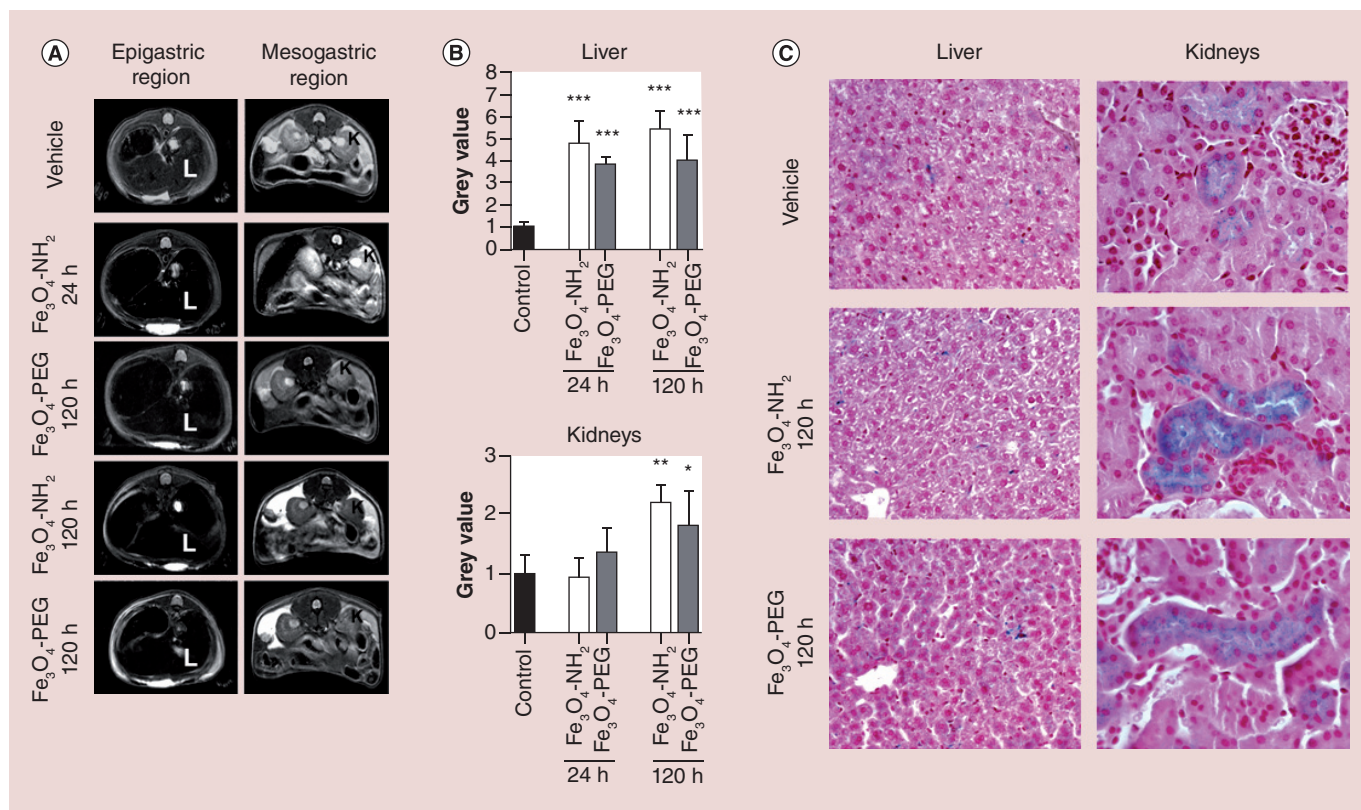| Nanoparticle	MTT	Trypan blue	*Xenopus laevis*
Quantum dot	xx	Xx	xx
PEG-Fe_3O_4	0	0	0
PS-COOH	0	0	xx
NH_2-Fe_3O_4	0	0	0

Figure 4. Assessment of iron oxide nanoparticles in a mammalian model. (A) Representative MRI images showing coronal slices corresponding to the epigastric (left column) and mesogatric region (right column). **(B)** Histograms showing the gray levels in liver (upper panel) and kidney (lower panel) measured from vehicle- (black bars), Fe_3O_4-NH_2 nanoparticles (NPs) (white bars) and Fe_3O_4-PEG NPs treated mice (gray bars) at 1 or 5 days after NP administration. Data are expressed as mean ± SD. *p < 0.005; **p < 0.01, ***p < 0.0001 compared with the vehicle (Student's t-test). **(C)** Perl's stained tissue sections from target organs in treated animals. Tissues counter-stained with eosin. Representative images shown. Higher power images to highlight normal tissue structure in the NP treated animals are shown in Supplementary Figure 8.
K: Kidneys; L: Liver.

and embryo assessment protocols (Tables 2 & 3). For this reason, we evaluated both these NPs in rodent models to confirm low toxicity. The other two NPs tested (PS-COOH and QD NPs) caused toxicity *in vivo* and therefore in our protocol would not progress to rodent model testing (Figure 1). We intravenously injected Fe_3O_4 NPs into mice and monitored where they accumulated in the animals using MRI to identify those organs exposed to the NPs. Darkening of signal was used as an indication of the presence of iron oxide NPs in organs, identifying the parenchyma of the kidneys and liver as target tissues for these NPs. Quantification of gray values confirmed the MRI scanning and suggests a prolonged permanence of NPs in liver, but potential clearance in the kidneys. Histochemical staining of the liver and kidneys was consistent with the MRI results, where crucially no histopathologies were induced in these organs by prolonged NP exposure. Positive Perl's staining was evident in liver of both Fe_3O_4-PEG and Fe_3O_4-NH_2 treated animals, which was detected as a cytoplasmic granular blue staining of scattered interstitial cells. In renal tissue of both Fe_3O_4-

PEG and Fe_3O_4-NH_2 treated animals staining within tubular epithelial cells was observed (Figure 4C). Neither presented with gross histopathological defects, demonstrating there was no cytotoxic effects of the iron core NPs in these organs. Crucially these results validated our findings from the integrated cell line and *X. laevis* toxicity assessment protocol, showing that the iron oxide NPs did not induce major effects in mammalian models.

Conclusion
Overall, we have developed a powerful integrative tool for screening nanomaterials that can work as bridge between *in vitro* and *in vivo* analysis for nanotoxicity. Our data demonstrate the flexibility of this multimodal preclinical assessment tool in the hazard assessment of nanomaterials, during the early stages of their production for biomedical applications. As such, functional modifications made to nanotherapeutics to enhance their efficacy, can be quickly analyzed using the protocol developed here for nanotoxic effects identified, which can then be addressed at an early stage in

development of the nanotherapy, prior to mammalian testing. This allows the rapid and cheap identification of possible NP-induced toxicities that may not be detectable through conventional cytotoxicity assays, at an early stage in the development of nanotherapeutics.

Future perspective

With the increase in development of nanotherapeutics and a lack of correlation between *in vitro* and *in vivo* safety assessment, there is now (more than ever) a need to develop standardized toxicity assessment protocols. We envisage that early developmental vertebrate models, such as *Xenopus,* can be easily integrated into a standardized safety protocol for novel nanomaterial testing, minimizing the time and cost of using mouse models and other higher vertebrates at an early stage in nanotherapeutic design. Furthermore, information gathered from *Xenopus* will help to understand the behavior of new nanomedicines in whole organism systems.

Ethical conduct of research

The authors state that they have obtained appropriate institutional review board approval or have followed the principles outlined in the Declaration of Helsinki for all human or animal experimental investigations. In addition, for investigations involving human subjects, informed consent has been obtained from the participants involved.

Executive summary

Xenopus laevis as a multiparametric nanotoxicity assessment tool
- We proposed *X. laevis* as a readily available laboratory model to develop a nanotoxicity screening tool and developed a simplified scoring system allowing us to easily and rapidly assess nanoparticle (NP) mediated toxicity in embryos at differing developmental stages.

Comparison of cytotoxicity & *X. laevis* data for hazard ranking of NPs
- The total scoring system combines cytotoxicity and *X. laevis* results for four different NPs for which a physical–chemical characterization in the biological environment was also performed

Assessment of NP safety in a mammalian system
- NPs with a low hazard ranking for the cell culture and embryo assessment protocols did not show major histopathologies in the organs where they were accumulated in mice, indicating a good prediction of *in vivo* NP effects.
- We developed a fast and cheap tool for screening nanomaterials that can work as bridge between *in vitro* and *in vivo* analysis for early stage screening of nanotoxicity.

References

Papers of special note have been highlighted as:
• of interest; •• of considerable interest.

1   Lee DE, Koo H, Sun IC, Ryu JH, Kim K, Kwon IC. Multifunctional nanoparticles for multimodal imaging and theragnosis. *Chem. Soc. Rev.* 41(7), 2656–2672 (2012).

2   Lewinski N, Colvin V, Drezek R. Cytotoxicity of nanoparticles. *Small* 4(1), 26–49 (2008).

3   Nystrom AM, Fadeel B. Safety assessment of nanomaterials: implications for nanomedicine. *J. Control. Release* 161(2), 403–408 (2012).

4   Hillegass JM, Shukla A, Lathrop SA, Macpherson MB, Fukagawa NK, Mossman BT. Assessing nanotoxicity

in cells *in vitro. Wiley Interdiscip. Rev. Nanomed. Nanobiotechnol.* 2(3), 219–231 (2010).

5   Duncan R. Nanomedicine(s) and their regulation: an overview. In: *Handbook of Safety Assessment of Nanomaterials – From Toxicological Testing to Personalized Medicine.* Fadeel B (Eds). Pan Stanford Publishing Pte Ltd (2013).

•   **Review of the challenges ahead for the safety of nanomedicines and their interaction in biological environments.**

6   Duncan R, Gaspar R. Nanomedicine(s) under the microscope. *Mol. Pharm.* 8(6), 2101–2141 (2011).

7   Venditto VJ, Szoka FC Jr. Cancer nanomedicines: so many papers and so few drugs! *Adv. Drug Deliv. Rev.* 65(1), 80–88 (2013).

8   Bawarski WE, Chidlowsky E, Bharali DJ, Mousa SA. Emerging nanopharmaceuticals. *Nanomedicine* 4(4), 273–282 (2008).

9   The International Council for Harmonisation of Technical Requirements for Pharmaceuticals for Human Use (ICH). www.ich.org

10 Krug HF, Wick P. Nanotoxicology: an interdisciplinary challenge. *Angew. Chem. Int. Ed. Engl.* 50(6), 1260–1278 (2011).

11 George S, Xia T, Rallo R *et al.* Use of a high-throughput screening approach coupled with *in vivo* zebrafish embryo screening to develop hazard ranking for engineered nanomaterials. *ACS Nano* 5(3), 1805–1817 (2011).

•• **Combining *in vitro* high-throughput toxicity assessment with a vertebrate model, Zebrafish, to create a comprehensive screening tool for engineered nanomaterials.**

12 Joris F, Manshian BB, Peynshaert K, De Smedt SC, Braeckmans K, Soenen SJ. Assessing nanoparticle toxicity in cell-based assays: influence of cell culture parameters and optimized models for bridging the *in vitro–in vivo* gap. *Chem. Soc. Rev.* 42(21), 8339–8359 (2013).

13 Liu Y, Liu B, Feng D *et al.* A progressive approach on zebrafish toward sensitive evaluation of nanoparticles' toxicity. *Integr. Biol. (Camb.)* 4(3), 285–291 (2012).

14 Bacchetta R, Moschini E, Santo N *et al.* Evidence and uptake routes for zinc oxide nanoparticles through the gastrointestinal barrier in *Xenopus laevis. Nanotoxicology* 8(7), 728–744 (2014).

15 Rizzo LY, Golombek SK, Mertens ME *et al. In vivo* nanotoxicity testing using the zebrafish embryo assay. *J. Mater. Chem. B* 1, doi:10.1039/C3TB20528B (2013).

16 Leconte I, Mouche I. Frog embryo teratogenesis assay on *Xenopus* and predictivity compared with *in vivo* mammalian studies. *Methods Mol. Biol.* 947 403–421 (2013).

•• **The use of *Xenopus* to assess teratogenic affects of potential pharmacutical compounds.**

17 Wheeler GN, Liu KJ. Xenopus: an ideal system for chemical genetics. *Genesis* 50(3), 207–218 (2012).

18 Schmitt SM, Gull M, Brandli AW. Engineering *Xenopus* embryos for phenotypic drug discovery screening. *Adv. Drug Deliv. Rev.* 69–70, 225–246 (2014).

19 Strober W. Trypan blue exclusion test of cell viability. In: *Current Protocols in Immunology.* Coligan JE (Ed.). John Wiley & Sons, Inc., A313.1–A313.2 (2001).

20 Berridge MV, Tan AS. Characterization of the cellular reduction of 3-(4,5-dimethylthiazol-2-yl)-2,5-diphenyltetrazolium bromide (MTT): subcellular localization, substrate dependence, and involvement of mitochondrial electron transport in MTT reduction. *Arch. Biochem. Biophys.* 303(2), 474–482 (1993).

21 Sherwood V, Chaurasiya SK, Ekstrom EJ *et al.* WNT5A-mediated beta-catenin-independent signalling is a novel regulator of cancer cell metabolism. *Carcinogenesis* 35(4), 784–794 (2014).

22 Tomlinson ML, Rejzek M, Fidock M, Field RA, Wheeler GN. Chemical genomics identifies compounds affecting *Xenopus laevis* pigment cell development. *Mol. Biosyst.* 5(4), 376–384 (2009).

23 Sherwood V, Manbodh R, Sheppard C, Chalmers AD. RASSF7 is a member of a new family of RAS association domain–containing proteins and is required for completing mitosis. *Mol. Biol. Cell* 19(4), 1772–1782 (2008).

24 Tarin D. Normal table of *Xenopus laevis* (Daudin). *J. Anatomy* 103(Pt 3), 578–578 (1968).

25 Bacchetta R, Tremolada P, Di Benedetto C *et al.* Does carbon nanopowder threaten amphibian development? *Carbon* 50(12), 4607–4618 (2012).

26 Bigini P, Diana V, Barbera S *et al.* Longitudinal tracking of human fetal cells labeled with super paramagnetic iron oxide nanoparticles in the brain of mice with motor neuron disease. *PLoS ONE* 7(2), e32326 (2012).

27 Canzi L, Castellaneta V, Navone S *et al.* Human skeletal muscle stem cell antiinflammatory activity ameliorates clinical outcome in amyotrophic lateral sclerosis models. *Mol. Med.* 18, 401–411 (2012).

28 OECD Environment, Health and Safety Publications, Series on the Safety of Manufactured Nanomaterials No=59 Presented at *Joint Meeting of the Chemicals Committee and the Working Party on Chemicals, Pesticides and Biotechnology 2015 (January).*

29 Tewari M, Wolf FW, Seldin MF, O'shea KS, Dixit VM, Turka LA. Lymphoid expression and regulation of A20, an inhibitor of programmed cell death. *J. Immunol.* 154(4), 1699–1706 (1995).

30 Filippi C, Pryde A, Cowan P *et al.* Toxicology of ZnO and TiO nanoparticles on hepatocytes: impact on metabolism and bioenergetics. *Nanotoxicology* 9(1), 126–134 (2015).

31 Hussain SM, Hess KL, Gearhart JM, Geiss KT, Schlager JJ. *In vitro* toxicity of nanoparticles in BRL 3A rat liver cells. *Toxicol. In Vitro* 19(7), 975–983 (2005).

32 Carlson C, Hussain SM, Schrand AM *et al.* Unique cellular interaction of silver nanoparticles: size-dependent generation of reactive oxygen species. *J. Phys. Chem. B* 112(43), 13608–13619 (2008).

33 Lowery LA, Sive H. Strategies of vertebrate neurulation and a re-evaluation of teleost neural tube formation. *Mech. Dev.* 121(10), 1189–1197 (2004).

34   Chan WH, Shiao NH. Cytotoxic effect of CdSe quantum dots on mouse embryonic development. *Acta Pharmacol. Sinica* 29(2), 259–266 (2008).

35   Nel A, Xia T, Madler L, Li N. Toxic potential of materials at the nanolevel. *Science* 311(5761), 622–627 (2006).

36   Pampaloni F, Reynaud EG, Stelzer EHK. The third dimension bridges the gap between cell culture and live tissue. *Nat. Rev. Mol. Cell Biol.* 8(10), 839–845 (2007).

37   Muller L, Riediker M, Wick P, Mohr M, Gehr P, Rothen-Rutishauser B. Oxidative stress and inflammation response after nanoparticle exposure: differences between human lung cell monocultures and an advanced three-dimensional model of the human epithelial airways. *J. R. Soc. Interface* 7, S27–S40 (2010).

38   Lee J, Lilly GD, Doty RC, Podsiadlo P, Kotov NA. *In vitro* toxicity testing of nanoparticles in 3D cell culture. *Small* 5(10), 1213–1221 (2009).

39   Movia D, Prina-Mello A, Bazou D, Volkov Y, Giordani S. Screening the cytotoxicity of single-walled carbon nanotubes using novel 3D tissue-mimetic models. *ACS Nano* 5(11), 9278–9290 (2011).

40   Astashkina AI, Jones CF, Thiagarajan G *et al.* Nanoparticle toxicity assessment using an *in vitro* 3-D kidney organoid culture model. *Biomaterials* 35(24), 6323–6331 (2014).

41   Smalley KM, Lioni M, Herlyn M. Life ins't flat: taking cancer biology to the next dimension. *In Vitro Cell. Devel. Biol. Animal* 42(8–9), 242–247 (2006).

42   Duan J, Yu Y, Shi H *et al.* Toxic effects of silica nanoparticles on zebrafish embryos and larvae. *PLoS ONE* 8(9), e74606 (2013).

43   Kim K-T, Zaikova T, Hutchison JE, Tanguay RL. Gold nanoparticles disrupt zebrafish eye development and pigmentation. *Toxicol. Sci.* 133(2), 275–288 (2013).

•   **Phenotypic toxicity study using embryos of a vertebrate model, Zebrafish, exposed to gold nanoparticles.**

44   Zhu X, Zhu L, Duan Z, Qi R, Li Y, Lang Y. Comparative toxicity of several metal oxide nanoparticle aqueous suspensions to Zebrafish (Danio rerio) early developmental stage. *J. Environ. Sci. Health Part A* 43(3), 278–284 (2008).

45   Walczyk D, Bombelli FB, Monopoli MP, Lynch I, Dawson KA. What the cell "sees" in bionanoscience. *J. Am. Chem. Soc.* 132(16), 5761–5768 (2010).

46   Liu G, Gao J, Ai H, Chen X. Applications and potential toxicity of magnetic iron oxide nanoparticles. *Small* 9(9–10), 1533–1545 (2013).

47   Shiohara A, Hoshino A, Hanaki K, Suzuki K, Yamamoto K. On the cyto-toxicity caused by quantum dots. *Microbiol. Immunol.* 48(9), 669–675 (2004).

48   Clancy AA, Gregoriou Y, Yaehne K, Cramb DT. Measuring properties of nanoparticles in embryonic blood vessels: towards a physicochemical basis for nanotoxicity. *Chem. Phys. Lett.* 488(4–6), 99–111 (2010).

49   Oslakovic C, Cedervall T, Linse S, Dahlback B. Polystyrene nanoparticles affecting blood coagulation. *Nanomedicine* 8(6), 981–986 (2012).

50   Dickinson AJ, Sive H. Development of the primary mouth in *Xenopus laevis*. *Dev. Biol.* 295(2), 700–713 (2006).

51   Marcon L, Riquet F, Vicogne D, Szunerits S, Bodart J-F, Boukherroub R. Cellular and *in vivo* toxicity of functionalized nanodiamond in *Xenopus* embryos. *J. Mater. Chem.* 20, 8064–8069 (2010).

52   Bacchetta R, Santo N, Fascio U *et al.* Nano-sized CuO, TiO(2) and ZnO affect *Xenopus laevis* development. *Nanotoxicology* 6(4), 381–398 (2012).